npg

ORIGINAL ARTICLE

Carbon and nitrogen fluxes associated with the cyanobacterium *Aphanizomenon* sp. in the Baltic Sea

Helle Ploug[1,3], Niculina Musat[2,3], Birgit Adam[2], Christina L Moraru[2], Gaute Lavik[2], Tomas Vagner[2], Birgitta Bergman[1] and Marcel MM Kuypers[2]

[1]*Department of Botany, Stockholm University, Stockholm, Sweden and* [2]*Department of Nutrient Group, Max Planck Institute for Marine Microbiology, Bremen, Germany*

Carbon and nitrogen fluxes in *Aphanizomenon* sp. colonies in the Baltic Sea were measured using a combination of microsensors, stable isotopes, mass spectrometry, and nanoscale secondary ion mass spectrometry (nanoSIMS). Cell numbers varied between 956 and 33 000 in colonies ranging in volume between 1.4×10^{-4} and $230 \times 10^{-4} \, mm^{-3}$. The high cell content and their productivity resulted in steep O_2 gradients at the colony–water interface as measured with an O_2 microsensor. Colonies were highly autotrophic communities with few heterotrophic bacteria attached to the filaments. Volumetric gross photosynthesis in colonies was 78 nmol $O_2 \, mm^{-3} \, h^{-1}$. Net photosynthesis was 64 nmol $O_2 \, mm^{-3} \, h^{-1}$, and dark respiration was on average 15 nmol $O_2 \, mm^{-3} \, h^{-1}$ or 16% of gross photosynthesis. These volumetric photosynthesis rates belong to the highest measured in aquatic systems. The average cell-specific net carbon-fixation rate was 38 and 40 fmol C $cell^{-1} \, h^{-1}$ measured by microsensors and by using stable isotopes in combination with mass spectrometry and nanoSIMS, respectively. In light, the net C:N fixation ratio of individual cells was 7.3 ± 3.4. Transfer of fixed N_2 from heterocysts to vegetative cells was fast, but up to 35% of the gross N_2 fixation in light was released as ammonium into the surrounding water. Calculations based on a daily cycle showed a net C:N fixation ratio of 5.3. Only 16% of the bulk N_2 fixation in dark was detected in *Aphanizomenon* sp. Hence, other organisms appeared to dominate N_2 fixation and NH_4^+ release during darkness.

Introduction

Aphanizomenon sp. is a filamentous, colony-forming N_2-fixing cyanobacterium, which frequently blooms in lakes and brackish waters. It occurs both as colonies and single trichomes during their growth, which often lasts 2–3 months during the summer in the Baltic Sea (Rolff *et al.*, 2007; Degerholm *et al.*, 2008). The primary productivity in the Baltic Sea by filamentous cyanobacteria, which are represented by *Aphanizomenon* sp., *Anabaena* sp., and *Nodularia spumigena*, represents 44% of the community primary production. These filamentous organisms comprise 20–30% of the cyanobacterial biomass in the Baltic Sea. The remaining primary productivity and biomass is represented by unicellular picocyanobacteria (Stal *et al.*, 1999; Stal and Walsby, 2000). In the absence of other nitrogen sources, these large filamentous cyanobacteria cover their nitrogen demand through N_2 fixation, and growth is probably limited by the availability of phosphate (Moisander *et al.*, 2003; Walve and Larsson, 2007). *Aphanizomenon* sp. accumulates inorganic phosphate during the growth season, and blooms appear to terminate when the internal storage is used up and bulk concentrations are low in mid-August in the Baltic Sea (Walve and Larsson, 2007).

N_2 fixation by filamentous cyanobacteria, including *Aphanizomenon* sp., is considered to be a quantitatively important source of nitrogen to the plankton community during the summer months in the Baltic Sea (Degerholm *et al.*, 2008). Nitrogen budgets of the Baltic Sea have suggested that *Aphanizomenon* leaks a substantial fraction of its fixed nitrogen that is used by other members (for example picocyanobacteria and heterotrophic bacteria) in the plankton community (Larsson *et al.*, 2001; Stal *et al.*, 2003; Rolff *et al.*, 2007).

C- and N-fluxes in *Aphanizomenon* sp.
H Ploug *et al*

2

Using stable isotopes, it was shown that 5–10% of the $^{15}N_2$ fixed by large cyanobacteria (*Aphanizomenon* sp. and *Nodularia* sp.) in the Baltic Sea is found in smaller organisms represented by the 2–5 μm size class, for example picocyanobacteria, after 8–10 h incubation time (Ohlendieck *et al.*, 2000). Direct measurements of ammonium or dissovled organic nitrogen (DON) release relative to N2-fixation rates, however, have not been performed in field-sampled cyanobacteria from the Baltic Sea.

Nanoscale secondary ion mass spectrometry (nanoSIMS) is a novel technique, which reveals elemental and isotopic surface composition after measurement of isotopic composition at a spatial resolution of 50 nm. Combining this technique with isotope enriched incubations has enabled measurements of N_2 and C fixation on a single-cell level in mixed populations (Musat *et al.*, 2008). Hence, using this technique we can now ascribe N_2 and C fixation to individual cells of different organisms in the Baltic Sea. To understand small-scale carbon and nitrogen fluxes in *Aphanizomenon* sp. colonies, we combined microsensors and stable isotope enrichment incubations with mass spectrometry as well as with nanoscale secondary ion mass spectrometry (nanoSIMS). Using microsensors, gross and net photosynthesis as well as dark respiration was measured directly in colonies as a function of colony size and cell content in field-sampled *Aphanizomenon* sp. in the Baltic Sea. Using stable isotope in combination with mass spectrometry and nanoSIMS, we measured carbon and nitrogen fixed by *Aphanizomenon* sp. cells and its release to the surrounding water.

Materials and methods

Sampling
In August 2008, *Aphanizomenon* colonies were sampled in the upper 10 m of the water column at station B1 (N 58° 48′ 28, E 17° 37′ 60) in the Stockholm archipelago using a plankton net (Hydro-bios: 0.5 m diameter, mesh size: 90 μm). Water at 5 m depth was collected by a water sampler. The salinity was 6 and the temperature was 19 °C. Samples were immediately brought to the laboratory in which they were analyzed by microsensors or incubated with stable isotopes.

Microscopy
All three dimensions of individual colonies were measured under a dissection microscope using a calibrated ocular micrometer. Their volume was calculated as ellipsoids: $Vol = 4/3\pi \times a \times b \times c$, where a, b, and c are the half-axes in the three dimensions. A microsensor was used to lift and turn colonies on an agar plate covered with water from the sampling site. Each colony with known size was thereafter collected using a wide bore pipette, transferred to an Eppendorf vial with 1.5 ml surrounding water, and fixed with a drop of 5% Lugol's solution. The fixed colonies were stored cold at 4 °C until further analysis. Colonies disintegrate in Lugol's solution, and the filaments sediment at the tip of the Eppendorf vial; 1 ml containing all filaments from each colony was pipetted into a gridded Sedgewick Rafter counting chamber (Wildlife supply Company). Numbers and dimensions of dispersed filaments, vegetative cells, and heterocyst frequency (in no filament per length, and in percent of vegetative cells) in each colony was measured under an inverted microscope (Zeiss, Switzerland) equipped with a digital camera (Axio Cam, Zeiss) connected to an image analysis program (AxioVision, Zeiss). Total cumulative filament length per field was measured until the mean value was stable and the s.d. was <2% of the mean value.

Total abundance of *Aphanizomenon* sp. trichomes and cells in bulk water and in concentrated samples (see below) was measured using the same counting procedure as described above. Five replicates, each comprising a subsample of 1 ml of 50 ml sample fixed in Lugol were analyzed both for *in situ* bulk water as well as concentrated samples.

Small-scale measurements of O_2 fluxes
Freshly sampled colonies were transferred to a Petri dish coated by a 3 mm thick agar layer (1% w:w) at the bottom and covered by filtered (0.2 μm) water from the sampling site. The diffusion coefficients of gases, ions, and solutes in 1% agar are close to those in (sea) water (Libicki *et al.*, 1988; Revsbech, 1989). Artifacts from a solid boundary, which limits solute exchange between colonies and the surrounding water, was, therefore, avoided by using a Petri dish coated with agar (Ploug and Grossart, 1999). The Petri dish was placed in a thermostated container at *in situ* temperature. Oxygen concentrations were measured at the colony–water interface using a Clark type oxygen microsensor (Revsbech, 1989) attached to a micromanipulator. The current was measured by a picoamperemeter (Unisense PA 2000) connected to a strip-chart recorder (Kipp and Zonen). The electrode was calibrated at anoxic conditions and at air saturation. Its 90% response time was <1 s and the stirring sensitivity <0.3%. The oxygen microelectrode tip was 2 μm wide and its position was observed under a dissection microscope with an ocular micrometer. The electrode was manually approached toward the colony until it visually touched the surface. Oxygen-concentration gradients were measured at the colony–water interface at 50 μm step increments. Three replicates of the O_2-concentration gradient were measured in light and in dark, respectively. The light source was a Schott lamp (KL 1500 LCD) equipped with an infra-red cutoff filter and calibrated using an LiCOR scalar irradiance sensor. The fluxes of oxygen were measured at steady state of concentration gradients

C- and N-fluxes in *Aphanizomenon* sp.
H Ploug *et al*

npg

3

at the colony–water interface, and calculated from Fick's first law of diffusion:

$$J = -D\frac{dC}{dr} \qquad (1)$$

where J is the flux ($nmol\,O_2\,cm^{-2}\,s^{-1}$), D is the diffusion coefficient of O_2 in the bulk water ($2.02 \times 10^{-5}\,cm^2\,s^{-1}$ at 6 and 19 °C; Broecker and Peng, 1974), and dC/dr is the radial-concentration gradient of O_2 ($nmol\,O_2\,cm^{-3}$). Surface area and volume was calculated as for ellipsoids (Mass, 1994). Carbon production rates were calculated assuming a photosynthetic quotient of $1.2\,mol\,O_2$: $1\,mol\,CO_2$.

Incubations with stable isotopes
Water samples containing 1.10×10^8 *Aphanizomenon* sp. cells per liter ($\pm 0.03 \times 10^8$ cells l^{-1}; s.e.) were incubated in 250 ml serum bottles by adding colonies harvested by the plankton net to bulk water samples. Microscopy revealed that the mean trichome size was $230 \pm 95\,\mu m$, and most heterocysts were observed within the trichomes. Hence, cells did not appear damaged by the sampling procedure. The serum bottles were closed with rubber stoppers through which ^{13}C bicarbonate was injected to a final bicarbonate concentration of $1.83\,mM$ (11% labeling) except for three control bottles. Using a gas mouse, 2 ml $^{15}N_2$ (Sigma, Germany) was injected to the sample (12% final labeling). The syringe was flushed several times with Argon gas between injections. All bottles were thoroughly shaken during 5 min to ensure an even distribution of dissolved $^{15}N_2$ in the samples. Many colonies remained intact, and microscopy did not reveal cell damage during this procedure. Three replicates were incubated for 0, 3, or 6 h in light at $300\,\mu mol$ photons $m^{-2}\,s^{-1}$, as measured using an LiCor scalar irradiance sensor, or in dark at *in situ* temperature (19 °C) in a thermostated room. The incubations were stopped by filtration of samples onto pre-combusted GF/F filters (for EA-MS analysis) (Montoya *et al.*, 1996). The filtrates were filled into 12 ml gas tight exetainers and killed by adding $100\,\mu l$ saturated $HgCl_2$ solution to each exetainer. Subsamples for nanoSIMS analysis were fixed with 2% paraformaldehyde and washed before filtration onto Gold-Palladium-coated GTTP filters (pore size, $0.22\,\mu m$; diameter 25 mm; Millipore, Germany).

EA-IRMS analysis
To determine the amount of ^{15}N gas and ^{13}C bicarbonate incorporated into biomass, water samples were filtered onto glass fiber filters and analyzed through mass spectrometry using N_2 and CO_2 released by flash combustion in excess oxygen at 1050 °C. An automated elemental analyzer coupled to a Delta Plus Advantage mass spectrometer was used (Montoya *et al.*, 1996). Before analysis, GF/F filters were freeze dried overnight and dehydrated in an HCl-smoke environment in a desiccator overnight. Round punchouts (Ø 1 cm) of the GF/F filters were packed into tin cups and were tightly pressed into a pill-shaped form. These were then loaded onto an autosampler flushed with helium, which automatically dropped the packed filters into the combustion furnace. As a standard, caffeine was used for calibration.

NanoSIMS analysis
For NanoSIMS analysis of single *Aphanizomenon* cells, Gold-Palladium-coated GTTP filters containing chemically fixed water samples were cut with a round stencil (Ø 5 mm) and mounted on a sample holder. The analysis was performed using a NanoSIMS 50 l manufactured by Cameca (Gennevilliers, France). For each individual cell, we recorded simultaneously secondary ion images of ^{12}C, ^{13}C, $^{12}C^{14}N$, and $^{12}C^{15}N$ using four electron multipliers. The measurements and the image and data processing were performed as described earlier (Musat *et al.*, 2008).

The $^{15}N/^{14}N$ and the $^{13}C/^{12}C$ ratios of individual *Aphanizomenon* cells were determined for experiments with and without (that is control experiments) labeled substrate. Subsequently, the $^{15}N/^{14}N$ and $^{13}C/^{12}C$ enrichment of individual cells was calculated by subtracting the average cellular ratios of *Aphanizomenon* in the control experiments from the ratios obtained for individual cells from the labeling experiment.

Ammonium analysis
The net release of $^{15}NH_4^+$ from cyanobacteria was quantified in the filtrate after the incubations with $^{15}N_2$ during 0, 3, and 6 h in light or darkness using the method by Warembourg (1993). Samples were analyzed on a GC-IR mass spectrometer (VG Isogas Limited, Middlewitch, UK).

The NH_4^+ microenvironment of colonies was modeled, knowing the diffusive properties of colonies from O_2 measurements, the net carbon fluxes, the C:N fixation ratio, and fraction of fixed nitrogen released as NH_4^+. We used an analytical diffusion model by Ploug *et al.* (1997), with a diffusion coefficient of NH_4^+ of $1.6 \times 10^{-5}\,cm^2\,s^{-1}$ at 6 and 19 °C (Li and Gregory, 1974).

Results

The number of cells in the *Aphanizomenon* sp. colonies was a significant function of colony volume (Figure 1). The largest colonies had a volume of $0.023\,mm^3$ with an equivalent spherical diameter of $340\,\mu m$, but most colonies were considerably smaller. The number of cells in individual colonies

C- and N-fluxes in *Aphanizomenon* sp.
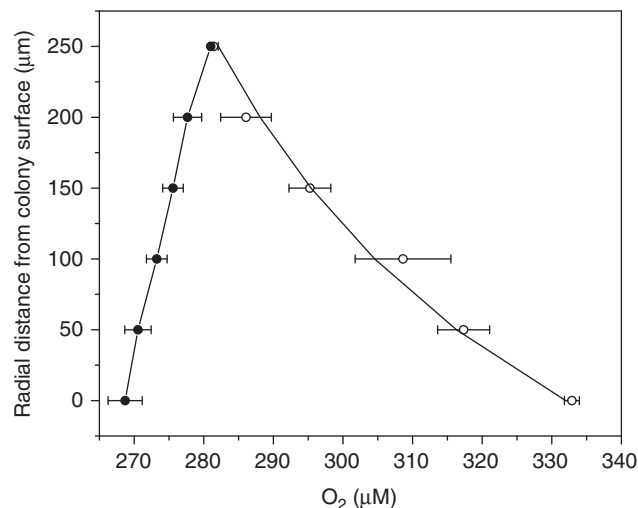H Ploug *et al*

4
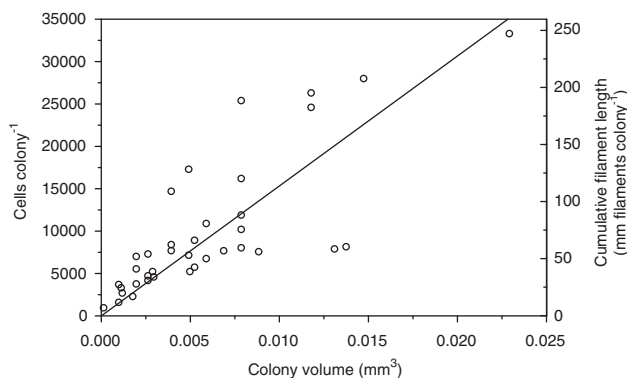
Figure 1 Number of cells and cumulative filament length (both shown as symbols) in *Aphanizomenon* colonies as a function of colony volume. The line represents linear regression between the variables (please see text).
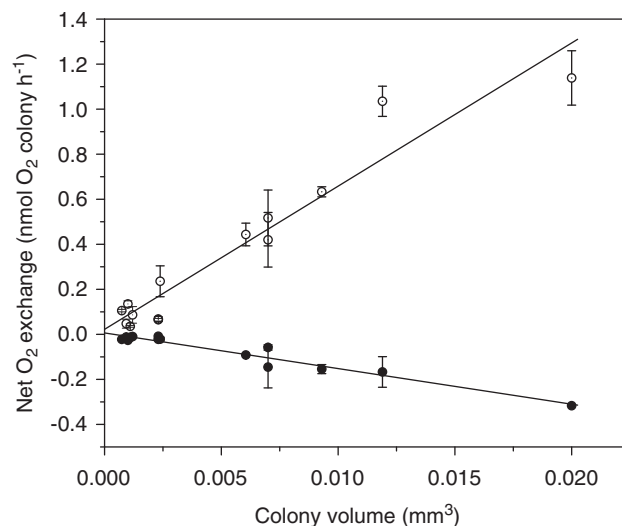

Figure 2 O_2 gradients measured at the colony–water interface during dark (closed symbols) and in light at $300 \mu mol$ photons $m^{-2} s^{-1}$ (open symbols). Each symbol represents the average value of three series of measurements with the s.d. of the mean value shown as bars. The curve represents the O_2-concentration gradient fitted to the measured values and used for flux calculations.

varied from 956 to 33 000 for colonies ranging between 1.4×10^{-4} and $230 \times 10^{-4} mm^3$ in volume. The average number of cells per colony was described as Cells $= 1.53 \times 10^6 \times (Vol_{col})$, where colony volume is measured in mm^3. Alternatively, biomass of filamentous cyanobacteria is measured as meter per length $(m l^{-1})$ (Hajdu *et al.*, 2007; Rolff *et al.*, 2007; Degerholm *et al.*, 2008). The cumulative length of filaments in individual colonies varied between 7 and 246 mm, and it was described by $L = 11 341 \times (Vol_{col})$; where length, L, is expressed in mm. The significance level was $R^2 = 0.61$; $n = 37$; $P < 0.0001$ for both expressions. The mean cell volume was $132 \mu m^3$, and the mean volume fraction occupied by cells in colonies was 0.19. Heterocysts were 1.5% of total cells or 2.02 ± 0.95 mm per filament independent of colony volume.

The cell content and their productivity in colonies gave rise to significant oxygen-concentration gradients at the colony–water interface (Figure 2). Oxygen concentrations at the colony surface varied up to $65 \mu M$ between the light $(300 \mu mol$ photons $m^{-2} s^{-1})$ and the dark exposed colonies (Figure 2). The gradients were measurable up to $200 \mu m$ from the surface of a $340 \mu m$ large colony. Net photosynthesis was 1.1 nmol colony^{-1} h^{-1}, and dark respiration was 0.3 nmol colony^{-1} h^{-1} as calculated from the oxygen gradients measured in light and dark, respectively. Hence, dark respiration was 22% of gross photosynthesis in this example.

The net photosynthesis and dark respiration measured as a function of colony size are shown (Figure 3). Net photosynthesis as well as dark respiration increased proportionally to colony volume. Net photosynthesis was described by NP $= 64 \times (Vol_{col})$; $R^2 = 0.92$ ($n = 14$; $P < 0.001$), and dark respiration was described by $R = -15 \times (Vol_{col})$; $R^2 = 0.94$ ($n = 14$; $P < 0.001$), where volume is measured as mm^3, and NP and R measured as nmol O_2 mm^{-3} h^{-1}. Thus, volume-specific gross photosynthesis, net photosynthesis, and dark respiration was 79, 64, and 15 nmol O_2 mm^{-3} h^{-1},


Figure 3 Net photosynthesis rate (open symbols) and dark respiration rate (closed symbols) measured as a function of colony volume. Each symbol represents the average value of three series of measurements with the s.d. of the mean value shown as bars.

respectively, independent of colony size. Combining these correlations with the biomass distribution (Figure 1), and assuming a cell-specific carbon content of $0.11 pg C \mu m^{-3}$ (Helcom, 1988) yielded a carbon-specific net photosynthesis rate of $0.029 h^{-1}$ and a dark respiration rate of $0.007 h^{-1}$ independent of colony size. Average cell-specific photosynthesis and respiration rates were 42 and 10 fmol O_2 cell^{-1} h^{-1} or 38 and 8.3 fmol C cell^{-1} h^{-1}, respectively, assuming a photosynthetic quotient of 1.2 (Table 1).

C- and N-fluxes in *Aphanizomenon* sp.
H Ploug *et al*

npg

5

Table 1 Net photosynthesis and dark respiration in *Aphanizomenon* sp.

Method	Net photosynthesis		Dark respiration	
	nmol C m⁻¹ h⁻¹	*fmol C cell⁻¹ h⁻¹*	*nmol C m⁻¹ h⁻¹*	*fmol C cell⁻¹ h⁻¹*
Microsensor[a]	5.4	38	−1.3	−8.3
NanoSIMS		40 ± 12	—	—

[a]Assuming a photosynthetic quotient of 1.2.
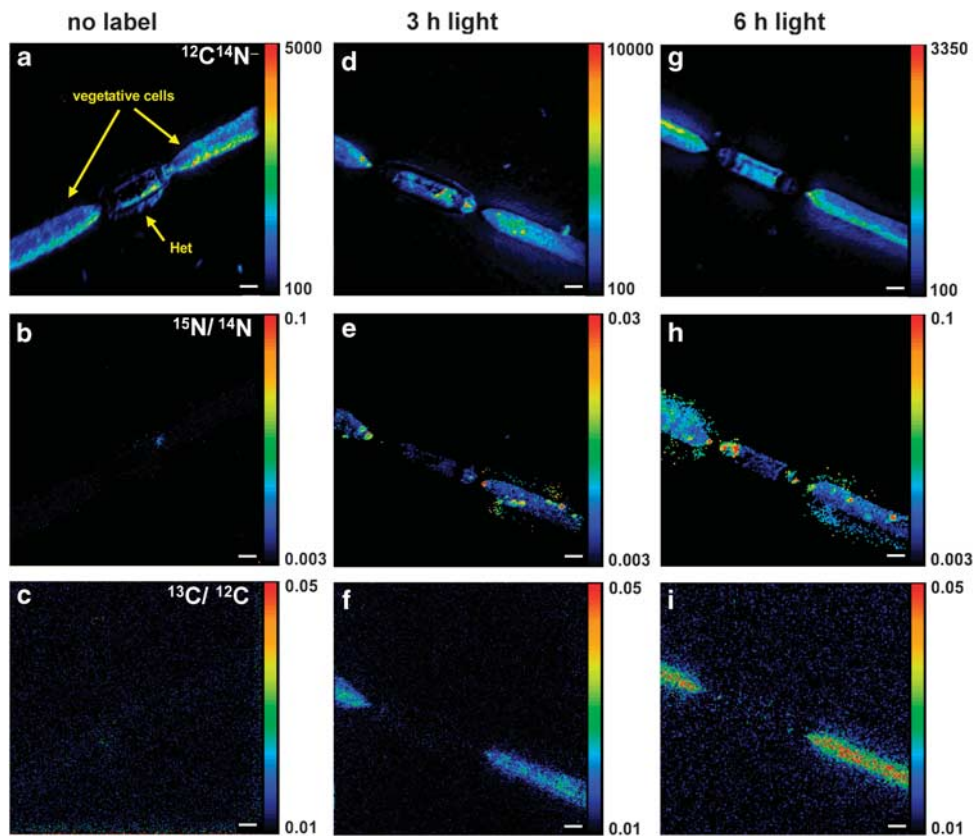
Figure 4 Distribution of $^{12}C^{14}N^-$ (**a**, **d**, **g**), and $^{15}N/^{14}N$ (**e**, **h**), and $^{13}C/^{12}C$ (**f**, **i**) in single *Aphanizomenon* cells as measured by nanoSIMS. **a–c**: no label, **d–f**: $t = 3$ h, **g–i**: $t = 6$ h. The size bars are 2 mm.

NanoSIMS analysis of colonies and filaments incubated with stable isotopes of C and N showed a rapid transfer of ^{15}N from heterocysts to vegetative cells. An example is shown in Figure 4. ^{13}C carbon was evenly distributed in vegetative cells after 3 h incubation time with only low assimilation into heterocysts. Heterocysts were also less enriched in ^{15}N as compared with vegetative cells. The occurrence of N-storage products, for example cyanophycin, was detectable after 3 h as regions with locally intense labeling of ^{15}N (in cyanophycin granules). Hence, incorporation of ^{15}N into proteins of heterocysts seemed low, and most of the ^{15}N label was transported to adjacent vegetative cells.

Cell-specific assimilation rates of ^{13}C and ^{15}N derived from nanoSIMS analysis and converted to total net C and total net N assimilated by using percent labeling are shown in the bulk in Figure 5. These varied largely between single cells after 6 h. Less C relative to N was incorporated into heterocysts as compared with vegetative cells. In vegetative cells, the average cell-specific carbon assimilation rate was 40 ± 12 fmol C cell⁻¹ h⁻¹, and the average cell-specific N assimilation into biomass was 4.8 ± 3.2 fmol N cell⁻¹ h⁻¹ in light. Hence, the average net C:N assimilation ratio into individual vegetative cells was 7.3 ± 3.4 in light (Table 2). Dark respiration was -8.3 fmol C cell⁻¹ h⁻¹ and dark net N_2-fixation rate was 0.28 ± 0.15 fmol N cell⁻¹ h⁻¹.

We tracked the release of fixed ^{15}N by measuring the production of $^{15}NH_4^+$ in the surrounding water (Table 2). The release of NH_4^+ was 35% of the total gross N_2 fixation in light. The corresponding value was 89% in darkness. The C:N ratio of gross

C- and N-fluxes in *Aphanizomenon* sp.
H Ploug *et al*

6

production (gross photosynthesis:gross N$_2$ fixation) was, therefore, 6.3 (Table 2). The NH$_4^+$ microenvironment of colonies was modeled, knowing the diffusive properties of colonies from O$_2$ measurements, the net carbon fluxes, the C:N fixation ratio, and fraction of fixed nitrogen released as NH$_4^+$. The NH$_4^+$-concentration gradients in a colony with O$_2$ gradients similar to the colony shown in Figure 2 are shown in Figure 6. The NH$_4^+$ concentration at the colony surface was 5.5 μM when the bulk concentration was 0.15 μM. Hence, ammonium was >37-fold enriched inside colonies as compared with the bulk water concentration.

Discussion

This study is the first to combine microsensors with mass spectrometry and nanoSIMS techniques to understand small-scale fluxes of carbon and nitrogen in a Baltic Sea cyanobacterium among those dominating the summer blooms. It was directly shown that *Aphanizomenon* is highly productive even during the late stage of its bloom and season in August. High concentrations of biomass in colonies and their productivity lead to significant O$_2$ gradients within these colonies and their surrounding water. The O$_2$ gradients measured during light

were similar to those reported in cultured colonies of *Aphanizomenon* sp. (Carlton and Pearl, 1989). Volume-specific gross photosynthesis was 79 nmol O$_2$ mm^{-3} h^{-1} independent of colony size. Hence, there was no indication of diffusion limitation of photosynthesis by CO$_2$ or bicarbonate in these colonies. Volume-specific gross photosynthesis was 10- to 80-fold higher than those measured in surface scums dominated by *Nodularia* sp. in the Baltic Sea (Ploug, 2008) and of other cyanobacterial surface blooms including *Aphanizomenon* in inland lakes (Ibelings and Maberly, 1998). This high rate is among the highest reported in aquatic systems, comparable with or higher than those measured in shallow sediments and microbial mats (Jørgensen *et al.*, 1983; Villbrant *et al.*, 1990; Lassen *et al.*, 1992).

Carbon-specific net photosynthesis rates were similar to optimal rates reported using the ^{14}C method in field-sampled *Aphanizomenon* from the Baltic Sea (Walve and Larsson, 2007) as well as in cultures of *Aphanizomenon* isolated from the Baltic Sea in the same area as that of this study (Degerholm *et al.*, 2006). The ^{14}C method provides an estimate of photosynthesis, which is usually considered to represent a rate between gross and net photosynthesis (that is the net carbon retainment in the cell). Using microsensors, it was possible to determine net
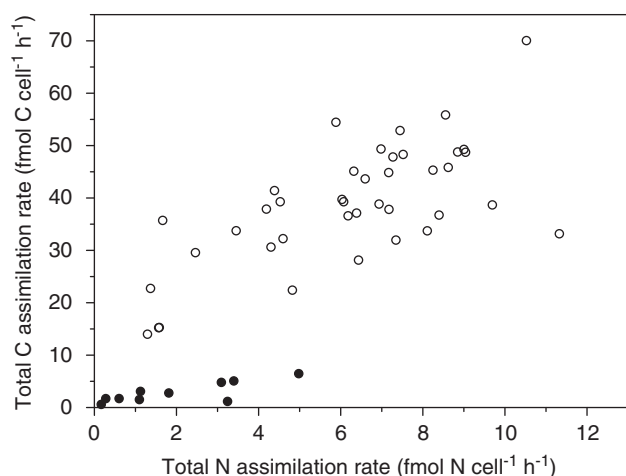
Figure 5 Cell-specific carbon and N$_2$-fixation rates as measured by nanoSIMS. Vegetative cells are shown as open symbols, and heterocysts as closed symbols.
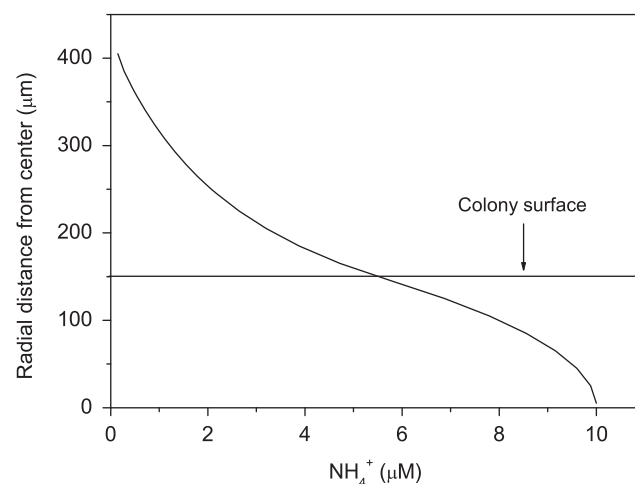
Figure 6 Ammonium gradient at colony–water interface of *Aphanizomenon* colony modeled from measured O$_2$ fluxes, C-, and N$_2$-fixation rates, and NH$_4^+$-release rates.

Table 2 Gross and net C:N fixation ratio, N$_2$-fixation rate, and net NH$_4^+$-release rate in *Aphanizomenon* sp. traced by ^{15}N

Gross C:N fixation ratio	Net C:N fixation ratio	N$_2$ net fixation rate (fmol N cell^{-1} h^{-1})[a]		NH$_4^+$-release rate (fmol N cell^{-1} h^{-1})	
Light	Light	Light	Dark	Light	Dark
6.3[b]	7.3 ± 3.4[c]	4.8 ± 3.2	0.28 ± 0.15	2.6	2.2

[a]Measured by nanoSIMS.
[b]Estimating from gross photosynthesis and gross N$_2$ fixation (net N$_2$ fixation+NH$_4^+$ release).
[c]Net C and net N$_2$ fixation in light of the same cells measured by nanoSIMS.

photosynthesis as well as dark respiration, and hence gross photosynthesis on single colonies of wild *Aphanizomenon* sp. Light microscopy of DAPI-stained colonies revealed that heterotrophic bacterial colonization of cyanobacterial filaments was low ($\sim$ 300 cells mm per filament; data not shown), as also indicated by the observation that dark respiration, similar to photosynthesis, was proportional to colony volume. Respiration was, therefore, mainly due to the cyanobacterium investigated. On average, it comprised 16% of gross photosynthesis, which partly reflects the cost of N_2 fixation. Cell-specific carbon assimilation rates compared well between rates obtained with microsensor techniques directly in colonies and the total C assimilation rates obtained from ^{13}C enrichment incubations.

NanoSIMS analysis showed a large variation of cell-specific net C and N assimilation. This has also been observed in natural populations of other phototrophic microorganisms (Musat *et al.*, 2008). Within trichomes, we measured a rapid transfer of fixed nitrogen from heterocysts to vegetative cells also reported in *Anabaena oscillarioides* cultures (Popa *et al.*, 2007). Generally, the ^{15}N label intensity in the heterocysts was low compared with that of the vegetative cells. However, a faint label was evident in this cell type already after 3 h, and a more distinct ^{15}N label after 6 h. This is particularly evident in the 'polar plugs,' composed of cyanophycin (arginine:aspartic acid in a 1:1 ratio), which are located at the vegetative cell junctions. Hence, although some of the nitrogen fixed is retained in the heterocysts, the newly synthesized products of N_2 fixation is primarily exported to the vegetative cells in which it apparently may be directed into three different routs: toward cellular growth, converted into cyanophycin (N storage), or being released extracellularly as ammonium to the environment. In Trichodesmium, the flow of fixed nitrogen into cyanophycin was also shown by nanoSIMS, and these granules may partly uncouple C and N_2 fixation from overall growth in cyanobacteria (Finzi-Hart *et al.*, 2009). Moreover, ammonium and DON release in *Trichodesmium* spp. may amount to $\sim$50% of N_2 fixation (Glibert and Bronk, 1994; Mulholland and Capone, 2001; Wannicke *et al.*, 2009).

The average net C:N assimilation ratio in single cells measured by nanoSIMS was 7.3 ± 3.4 in light, and a large fraction (35%) of the newly fixed N was released as ammonium to the surrounding water. Hence, gross N_2 fixation was approximately 1.5-fold higher than net N_2 fixation. Gross C:N fixation estimated from gross photosynthesis and gross N_2 fixation was 6.3 (Table 2). In the Baltic Sea, the C:N ratio of large ($>20\,\mu m$) cyanobacteria varies between 6 and 20 (Degerholm *et al.*, 2008). The net C:N fixation ratio varies largely between 1 and 40 presumably because of a variable NH_4^+ release by the large cyanobacteria (Gallon *et al.*, 2002). Net C- and N-fixation rates by large cyanobacteria are, therefore, not always closely coupled in the Baltic Sea. Our estimates of gross and net C:N fixation rates

in light, however, were close to a C:N ratio of 6.6. A high release of DOC or respiration of C could be expected to maintain a lower somatic C:N ratio, when the C:N fixation ratio is high. Such high DOC release as reflected by a large difference between rates obtained with isotopes, which are incubated for 6 h, and those obtained using the microsensor technique, which measures instantaneous photosynthesis, was not observed in our study and has also not been reported elsewhere. *Aphanizomenon* sp. seldom occurs in the uppermost water column, in which incident light intensities are highest (Hajdu *et al.*, 2007). Integration over a day–night cycle of 10 h:14 h at 3–4 m depth (Secchi depth was 6 m, only) resulted in a lower net C:N fixation ratio of $(10 \times 38 – 14 \times 8.3){:}(10 \times 4.8 + 14 \times 0.28) = 5.1$, because N_2-fixation rate is reduced and carbon is respired during night.

We are not aware of any reports on endogenous rhythms of C and N_2 fixation in *Aphanizomenon* sp. as reported for *Trichodesmium* (Berman-Frank *et al.*, 2001; Wannicke *et al.*, 2009). However, net N_2 fixation by *Aphanizomenon* sp. was 17-fold lower during darkness as compared with that in light. Combined NanoSIMS and EA-IRMS analysis of ^{15}N uptake showed that N_2 fixation by *Aphanizomenon* sp. represented 78% and 16% of the bulk N_2 fixation during light and darkness, respectively. Hence, $^{15}N_2$ fixation and the high $^{15}NH_4^+$ release in the bulk during darkness can thus partly be ascribed to other N_2-fixing organisms.

Our study directly shows that *Aphanizomenon* sp. leaks a substantial fraction of its fixed nitrogen as ammonium to the surrounding water. Leakage of ammonium, however, could partly be due to breakage of cells during the incubations and filtration procedures or because of lysed cells. Microscopic analysis and nanoSIMS images did not reveal a significant number of broken cells. A recent study using alternative techniques without potential filtration artifacts has shown a similar high light-dependent ammonium release in *Nodularia* sp. in the Baltic Sea (Ploug and Adam, unpublished). In this study, modeled NH_4^+ concentrations inside *Aphanizomenon* colonies were 37-fold higher than that of the bulk (Figure 6), and such colonies could potentially be a microenvironment favorable for growth of heterotrophic bacteria. Many pelagic bacteria are motile, show chemotaxis toward aggregate nutrient sources, and their colonization times are in the order of minutes (Kiørboe *et al.*, 2002). However, bacterial colonization of *Aphanizomenon* colonies was low (data not shown). O_2 gradients measured during dark were also less steep as compared with those measured in cultured colonies (Carlton and Pearl, 1989). Lower abundance of attached bacteria on *Aphanizomenon* colonies than on *Nodularia* sp. has been observed earlier in the Baltic Sea (Ulla Rasmussen and B Bergman, unpublished). The reason as to why *Aphanizomenon* filaments are poorly colonized by heterotrophic bacteria is

C- and N-fluxes in *Aphanizomenon* sp.
H Ploug *et al*

8

unclear, but may be explained by release of secondary metabolites with high concentrations inside colonies similar to the high concentrations of O_2 and ammonium during light as shown here.

During summer, *Aphanizomenon* sp. occurs at average abundances up to $20\,ml^{-1}$ in the upper 20 m of the water column with peaks around $40–60\,ml^{-1}$ in the Baltic Sea (Hajdu *et al.*, 2007; Rolff *et al.*, 2007; Degerholm *et al.*, 2008). This abundance may be represented by 200–300 average-sized colonies per liter (Figure 1). Buoyancy in *Aphanizomenon* is controlled by the numerous gas vesicles forming larger gas vacuoles that may occupy a large proportion of the vegetative cell volume. In addition, colony formation increases the buoyancy capacity over that held by single filaments (Reynolds and Walsby, 1975). This is supported by the observation that cell fraction volumes in colonies on average are as high as 0.19 as measured in this study. Using this buoyancy capacity, colonies can position themselves at favorable light and/or nutrient conditions in the water column to capture the energy needed for N_2 fixation through photosynthesis during day and migrate below the pycnocline at night presumably to take up other nutrients, for example ortophosphate (Reynolds and Walsby, 1975; Walsby *et al.*, 1997; Hajdu *et al.*, 2007).

Combining all measurements, we can make a budget of the small-scale fluxes of carbon and nitrogen in *Aphanizomenon* sp. For each mole carbon fixed at saturating light intensity, 0.16 was respired and $0.16\,mol\ N_2$ was fixed of which 0.05 mol was released as NH_4^+ to the surrounding water. Our study also showed that net C and N assimilation by *Aphanizomenon* sp. was $5.4\,nmol\,C\,m^{-1}\,filament\,h^{-1}$ and $0.74\,nmol\,N\,m^{-1}\,filament\,h^{-1}$, respectively, at saturating light intensities, and $-1.3\,nmol\,C\,m^{-1}\,filament\,h^{-1}$ and $0.04\,nmol\,N\,m^{-1}\,filament\,h^{-1}$, respectively, in darkness. Extrapolating these data back to the Baltic Sea and assuming an average abundance of *Aphanizomenon* sp. of $20\,ml^{-1}$ in the upper 4 m water column (Hajdu *et al.*, 2007; Degerholm *et al.*, 2008), these rates correspond to $108\,nmol\,C\,l^{-1}\,h^{-1}$ and $15\,nmol\,N\,l^{-1}\,h^{-1}$ at saturating light intensities, and $-26\,nmol\,C\,l^{-1}\,h^{-1}$ and $0.86\,nmol\,N\,l^{-1}\,h^{-1}$ during darkness. Integrating the net C fixation and net N_2 fixation by *Aphanizomenon* sp. in the upper 4 m assuming saturating light intensities during 10 h light and 14 h darkness yields a net C assimilation rate of $2.9\,mmol\,C\,m^{-2}$ per day, and a net N_2 fixation rate of $0.55\,mmol\,N\,m^{-2}$ per day for only *Aphanizomenon* sp. In this calculation, dark respiration consumes approximately 50% of the C fixed during daytime, and net N_2 fixation during dark comprises 10% of the total, daily net N_2 fixation, only. The estimate of daily net N_2 fixation is close to the average measured value of integrated N_2-fixation rate by cyanobacteria ($>20\,\mu m$) occurring at an average abundance of $20\,ml^{-1}$ in the Baltic Sea (Degerholm *et al.*, 2008). Considering that *Aphanizomenon* sp. blooms approximately 60–90 days

per year, our measurements suggest that its potential net N_2 fixation may be in the order of $30–45\,mmol\,N_2\,m^{-2}$ per year, and the gross N_2 fixation may be at least up to $70\,mmol\,N_2\,m^{-2}$ per year (excluding NH_4^+ release during darkness). During a 3-year study, N_2 fixation by cyanobacteria ($>20\,\mu m$) in the Baltic Sea was recently reported to range between 21 and $78\,mmol\,N\,m^{-2}$ per year, and it contributed between 64% and 88% to total N_2 fixation measured at the same stations. (Degerholm *et al.*, 2008). Cyanobacterial blooms are characterized by high spatial and temporal variability in the Baltic Sea, and local concentrations of *Aphanizomenon* sp. can vary considerably, for example from 2 to $60\,ml^{-1}$ during summer (Hajdu *et al.*, 2007; Rolff *et al.*, 2007; Degerholm *et al.*, 2008). Local N_2 fixation by large cyanobacteria, therefore, varies depending on their abundance, physiological conditions, and chemical/physical parameters in the water column. Budget calculations of inorganic nitrogen in the Baltic Sea indicate that total N_2-fixation rates range between 60 to $140\,mmol\,N\,m^{-2}$ per year (Larsson *et al.*, 2001). ^{15}N tracer studies suggest N_2-fixation rates to range between 101 and $263\,mmol\,N\,m^{-2}$ per year (average: $125\,mmol\,N\,m^{-2}$ per year) (Wasmund *et al.*, 2001). On the basis of our study, we can conclude that *Aphanizomenon* sp. contributes significantly to the overall N_2 fixation of which a substantial fraction is directly released as NH_4^+ into the surrounding water. *Aphanizomenon* sp. thus seems to be a significant player in large-scale carbon and nitrogen biogeochemical fluxes in the Baltic Sea.

Acknowledgements

References

Berman-Frank I, Lundgren P, Chen YB, Kupper H, Kolber Z, Bergman B *et al.* (2001). Segregation of nitrogen fixation and oxygenic photosynthesis in the marine cyanobacterium *Trichodesmium*. *Science* **294**: 1534–1537.

Broecker WS, Peng TH. (1974). Gas exchange rates between air and sea. *Tellus* **26**: 21–35.

Carlton RG, Pearl HW. (1989). Oxygen induced changes in morphology of aggregates of *Aphanizomenon flos-aquae* (Cyanophyceae): implications for nitrogen fixation potentials. *J Phycol* **25**: 326–333.

Degerholm J, Gundersen K, Bergman B, Söderbäck E. (2006). Phosphorus-limited growth dynamics in two

C- and N-fluxes in *Aphanizomenon* sp.
H Ploug *et al*

9

Baltic Sea cyanobacteria, *Nodularia* sp. and *Aphanizomenon* sp. *FEMS Microbiol Ecol* **58**: 323–332.

Degerholm J, Gundersen K, Bergman B, Söderbäck E. (2008). Seasonal significance of N_2 fixation in coastal and offshore waters of the northwestern Baltic Sea. *Mar Ecol Prog Ser* **360**: 73–84.

Finzi-Hart JA, Pett-Ridge J, Weber PK, Popa R, Fallon SJ, Gunderson T *et al.* (2009). Fixation and fate of C and N in the cyanobacterium *Trichiodesmium* using nanometer-scale secondary ion mass spectrometry. *Proc Natl Acad Sci* **106**: 6345–6350.

Gallon JR, Evans AM, Jones DA, Albertano P, Congestri R, Bergman B *et al.* (2002). Maximum rates of N_2 fixation and primary production are out of phase in a developing cyanobacterial bloom in the Baltic Sea. *Limnol Oceanogr* **47**: 1514–1521.

Glibert PM, Bronk DA. (1994). Release of dissolved organic nitrogen by marine diazotrophic cyanobacteria, Trichodesmium spp. *Appl Environ Microbiol* **60**: 3996–4000.

Hajdu S, Höglander H, Larsson U. (2007). Phytoplankton vertical distributions and composition in Baltic Sea cyanobacterial blooms. *Harmful Algae* **6**: 189–205.

Helcom (Helsinki commission) (1988). *Guidelines for the Baltic Monitoring Programme for the Third Stage, Part D. Biological Determinants*. Balt Sea Environ Proc 27 D, Baltic Marine Environment Protection Commission: Helsinki, pp 23–54.

Ibelings BW, Maberly SC. (1998). Photoinhibition and the availability of inorganic carbon restrict photosynthesis by surface blooms of cyanobacteria. *Limnol Oceanogr* **43**: 408–419.

Jørgensen BB, Revsbech NP, Cohen Y. (1983). Photosynthesis and structure of benthic microbial mats: microelectrode and s.e.m. studies of four cyanobacterial communities. *Limnol Oceanogr* **28**: 1075–1093.

Kiørboe T, Grossart H-P, Ploug H, Tang K. (2002). Mechanisms and rates of bacterial colonization of sinking aggregates. *Appl Environ Microbiol* **68**(8): 3996–4006.

Larsson U, Hajdu S, Walve J, Elmgren R. (2001). Baltic Sea nitrogen fixation estimated from the summer increase in upper mixed layer total nitrogen. *Limnol Oceanogr* **46**: 811–820.

Lassen C, Ploug H, Jørgensen BB. (1992). Microalgal photosynthesis and spectral scalar irradiance in coastal marine sediments of Limfjorden, Denmark. *Limnol Oceanogr* **37**: 760–772.

Libicki SB, Salmon PM, Robertson CR. (1988). The effective diffusive permeability of a nonreacting solute in microbial cell aggregates. *Biotechnol Bioeng* **32**: 68–85.

Li Y-H, Gregory S. (1974). Diffusion of ions in sea water and in deep-sea sediments. *Geochim Cosmochim Acta* **38**: 703–714.

Mass LRM. (1994). On the surface area of an ellipsoid and related integrals of elliptic integrals. *Comput Appl Math* **51**: 237–249.

Moisander PH, Steppe TF, Hall NS, Kuparinen J, Pearl HW. (2003). Variability in nitrogen and phosphorus limitation for Baltic Sea phytoplankton during nitrogen-fixing cynobacteria blooms. *Mar Ecol Prog Ser* **262**: 81–95.

Montoya JP, Voss M, Kahler P, Capone DG. (1996). A simple, high-precision, high-sensitivity tracer assay for N2 fixation. *Appl Environ Microb* **62**: 986–993.

Mulholland MR, Capone DG. (1996). Stoichiometry of nitrogen utilization in cultured populations of *Trichodesmium* IMS101: implications for growth. *Limnol Oceanogr* **46**: 436–443.

Musat N, Halm H, Winterholler B, Hoppe P, Peduzzi S, Hillion F *et al.* (2008). A single-cell view on the ecophysiology of anaerobic phototrophic bacteria. *PNAS* **105**: 17861–17866.

Ohlendieck U, Stuhr A, Siegmund H. (2000). Nitrogen fixation by diazotrophic cyanobacteria in the Baltic Sea and transfer of the newly fixed nitrogen to picoplankton organisms. *J Mar Sys* **25**: 213–219.

Ploug H. (2008). Cyanobacterial aggregates formed by *Aphanizomenon* sp. and *Nodularia spumigena* in the Baltic Sea: small-scale fluxes, pH and oxygen microenvironments. *Limnol Oceanogr* **53**: 914–921.

Ploug H, Grossart H-P. (1999). Bacterial production and respiration in suspended aggregates—a matter of the incubation method. *Aquat Microb Ecol* **20**: 21–29.

Ploug H, Kühl M, Buchholz B, Jørgensen BB. (1997). Anoxic aggregates—an ephemeral phenomenon in the ocean. *Aquat Microbol Ecol* **13**: 285–294.

Popa R, Weber PK, Pett-Ridge J, Finzi JA, Fallon SJ, Hutcheon ID *et al.* (2007). Carbon and nitrogenfixation and metabolite exchange in and between individual cells of Anabaena oscillarioides. *ISME J* **1**: 354–360.

Revsbech NP. (1989). An oxygen microelectrode with a guard cathode. *Limnol Oceanogr* **34**: 474–478.

Reynolds CV, Walsby AE. (1975). Water blooms. *Biol Rev* **50**: 437–481.

Rolff C, Almesjö L, Elmgren R. (2007). Nitrogen fixation and abundance of the diazotrophic cyanobacterium *Aphanizomenon* sp. in the Baltic Proper. *Mar Ecol Prog Ser* **332**: 107–118.

Stal LJ, Albertano P, Bergman B, von Bröckel K, Gallon JK, Hayes PK *et al.* (2003). BASIC: Baltic Sea Cyanobacteria. An investigation of the structure and dynamics of water blooms of cyanobacteria in the Baltic Sea-resposes to a changing environment. *Cont Shelf Res* **23**: 1695–1714.

Stal LJ, Walsby AE. (2000). Photosynthesis and nitrogen fixation in a cyanobacterial bloom in the Baltic Sea. *Eur J Phycol* **35**: 97–108.

Stal LJ, Staal M, Villbrandt M. (1999). Nutrient control of cyanobacterial blooms in the Baltic Sea. *Mar Ecol Prog Ser* **18**: 165–173.

Villbrant M, Stal LJ, Krumbein WE. (1990). Interactions between nitrogen fixation and oxygenic photosynthesis in a marine cyanobacterial mat. *FEMS Microb Ecol* **74**: 59–72.

Walve J, Larsson U. (2007). Blooms of Baltic Sea *Aphanizomenon* sp.(Cyanobacteria) collapse after internal phosphorus depletion. *Aquat Microb Ecol* **49**: 57–69.

Walsby AE, Hayes PK, Boje R, Stal L. (1997). The selective advantage of buoyancy provided by gas vesicles for planktonic cyanobacteria in the Baltic Sea. *New Phytol* **136**: 407–417.

Wannicke N, Koch BP, Voss M. (2009). Release of fixed N_2 and C as dissolved compounds by *Trichodesmium erythreum* and *Nodularia spumigena* under the influence of high light and high nutrient (P). *Aquat Microb Ecol* **57**: 175–189.

Warembourg FR. (1993). Nitrogen isotopes techniques. In: Knowles K., Blackburn TH (eds). *Nitrogen Fixation in Soil and Plant Systems*. Academic: New York. pp 157–180.

Wasmund N, Voss M, Lochte K. (2001). Evidence of nitrogen fixation by non-heterocystous cyanobacteria in the Baltic Sea and re-calculation of a budget of nitrogen fixation. *Mar Ecol Prog Ser* **214**: 1–14.